



Cite this: *Phys. Chem. Chem. Phys.*,  
2014, 16, 21524

## Identification of adsorbed molecules via STM tip manipulation: CO, H<sub>2</sub>O, and O<sub>2</sub> on TiO<sub>2</sub> anatase (101)†

Martin Setvin,<sup>\*a</sup> Benjamin Daniel,<sup>a</sup> Ulrich Aschauer,<sup>bc</sup> Weiyi Hou,<sup>b</sup> Ye-Fei Li,<sup>b</sup> Michael Schmid,<sup>a</sup> Annabella Selloni<sup>b</sup> and Ulrike Diebold<sup>a</sup>

While Scanning Tunneling Microscopy (STM) has evolved as an ideal tool to study surface chemistry at the atomic scale, the identification of adsorbed species is often not straightforward. This paper describes a way to reliably identify H<sub>2</sub>O, CO and O<sub>2</sub> on the TiO<sub>2</sub> anatase (101) surface with STM. These molecules are of a key importance in the surface chemistry of this and many other (photo-) catalytic materials. They exhibit a wide variety of contrasts in STM images, depending on the tip condition. With clean, metallic tips the molecules appear very similar, *i.e.*, as bright, dimer-like features located in the proximity of surface Ti<sub>5c</sub> atoms. However, each species exhibits a specific response to the electric field applied by the STM tip. It is shown that this tip–adsorbate interaction can be used to reliably ascertain the identity of such species. The tip–adsorbate interactions, together with comparison of experimental and calculated STM images, are used to analyse and revisit the assignments of molecular adsorbed species reported in recent studies.

Received 20th July 2014,  
Accepted 8th August 2014

DOI: 10.1039/c4cp03212h

[www.rsc.org/pccp](http://www.rsc.org/pccp)

### Introduction

Titanium dioxide is a technologically important material used in various applications including catalysis,<sup>1</sup> photocatalysis,<sup>2</sup> and electrochemical (Grätzel) solar cells.<sup>3</sup> It is also of high interest in emerging areas of electronics.<sup>4,5</sup> TiO<sub>2</sub> crystallizes in several forms; the technologically relevant phases are rutile (thermodynamically stable) and anatase (metastable).<sup>6</sup> Anatase is more relevant for applications for two reasons. First, TiO<sub>2</sub> nanomaterials grow preferentially in the anatase phase due to the low surface energy of the (101) plane.<sup>7</sup> Second, anatase turns out to be more efficient for many applications. The reasons of this higher efficiency have been intensively debated in recent years.<sup>8–10</sup>

Scanning Tunneling Microscopy (STM) is a method frequently used for investigating adsorbed molecules. The main advantage of the method is its ability to directly provide local information with atomic-scale resolution. STM is sensitive to the geometry and the electronic structure of the adsorbed species, but provides very limited information on the chemical identity. While

spectroscopic techniques are, of course, very useful for complementary measurements, they typically average over a wide area. The identification of an adsorbed species at one specific site usually relies on a subtle comparison of experimentally measured STM images to Density Functional Theory (DFT) calculations. This procedure is complicated by the fact that experimentally-obtained STM images may be tip-dependent; different tip terminations often provide varying contrasts in scanning probe microscopy.<sup>11,12</sup> This effect is more or less pronounced, depending on the particular surface–adsorbate system.

The simple molecules H<sub>2</sub>O, CO and O<sub>2</sub> are of key importance in chemistry-related applications of TiO<sub>2</sub>.<sup>1,2,6,9,13,14</sup> When adsorbed on the TiO<sub>2</sub> anatase (101) surface, a rich variety of contrasts is encountered in STM images. Often these molecules show a very similar appearance, *i.e.*, a dimer-like feature located in proximity of a surface Ti<sub>5c</sub> atom. It is thus difficult to unambiguously identify these molecules solely from STM images. However, they are influenced by the STM tip at specific scanning conditions, *i.e.* high sample bias and/or tunneling out of filled states. These (irreversible) tip–adsorbate interactions provide a reliable way to identify each of these adsorbates.

<sup>a</sup> Institute of Applied Physics, Vienna University of Technology, Wiedner Hauptstrasse 8-10/134, 1040 Wien, Austria. E-mail: setvin@iap.tuwien.ac.at

<sup>b</sup> Department of Chemistry, Princeton University, Frick Laboratory, Princeton, NJ 08544, USA

<sup>c</sup> Materials Theory, ETH Zurich, Wolfgang-Pauli-Strasse 27, 8093 Zürich, Switzerland

† Electronic supplementary information (ESI) available. See DOI: 10.1039/c4cp03212h

### Materials and methods

The experiments were performed in an Ultra High Vacuum (UHV) chamber with a base pressure below  $1 \times 10^{-9}$  Pa, equipped with a

commercial Omicron LT-STM head. Electrochemically etched W STM tips were cleaned by  $\text{Ar}^+$  sputtering and treated on a Au(110) surface to obtain a reproducible, metallic tip condition. A mineral anatase sample was cleaved<sup>15</sup> and cleaned *in situ* by cycles of  $\text{Ar}^+$  sputtering and annealing.<sup>16</sup> A detailed analysis of impurity levels in the crystal is given in ref. 13.

The DFT calculations were carried out within the plane wave pseudopotential scheme using the Perdew–Burke–Ernzerhof (PBE)<sup>17</sup> functional and PBE augmented by on-site Coulomb repulsion (PBE +  $U$ )<sup>18</sup> as implemented in the QUANTUM ESPRESSO package.<sup>19</sup> We used ultra-soft pseudopotentials<sup>20</sup> with Ti 3s, 3p and Nb 4s, 4p semicore states treated explicitly. Wave functions were expanded in plane-waves with a kinetic energy cutoff of 30 Ry and 300 Ry for the smooth and augmented part of the density, respectively. On-site Coulomb repulsion parameters  $U = 3.5$  eV on Ti 3d and  $U = 0.8$  eV on Nb 4d were determined from first principles linear response.<sup>21,22</sup>

The anatase (101) surface was modeled using a repeated slab geometry. Each slab had three  $\text{TiO}_2$  layers corresponding to a thickness of 9.7 Å and consecutive slabs were separated by a 10 Å vacuum gap. A  $3 \times 1$  ( $10.26 \times 11.31$  Å<sup>2</sup>) surface supercell was considered. Due to the large size of this supercell, reciprocal space sampling was restricted to the  $\Gamma$  point. For geometry optimizations we used the Broyden–Fletcher–Goldfarb–Shanno (BFGS) scheme until forces converged below 0.05 eV Å<sup>-1</sup>.

## Results

### Water

Water adsorbs non-dissociatively on the anatase (101) surface.<sup>14,23</sup> Its O atom binds to a 5-fold coordinated surface Ti atom ( $\text{Ti}_{5c}$ ), while the H atoms form hydrogen bonds with the two neighboring surface  $\text{O}_{2c}$  atoms (ref. 14, also see Fig. 1d). The calculated adsorption energy of  $\text{H}_2\text{O}$  is 730 meV,<sup>14</sup> consistent with temperature programmed desorption spectra, which show a broad water desorption peak centered at  $\sim 250$  K.<sup>23</sup>

In STM images water molecules are observed with two distinctly different appearances. Fig. 1a and b show the anatase (101) surface with a small coverage of water. The arrows point out single molecules. As clearly seen in the insets these appear as either bright, extended features, or as three consecutive, bright–dark–bright spots. The difference in the image contrast in Fig. 1a and b does *not* originate from a different sample bias or tunneling current, however. Each of these contrasts is specific for a certain tip condition. The molecules' appearance in Fig. 1a is typical for clean, metallic tips; in this case the appearance does not depend strongly on the sample bias. It shows agreement with the calculated STM contrast (see Fig. 1e). The contrast in Fig. 1b was frequently encountered for sample temperatures in the range from 180 to 220 K; at conditions where thermal diffusion of water molecules across the surface

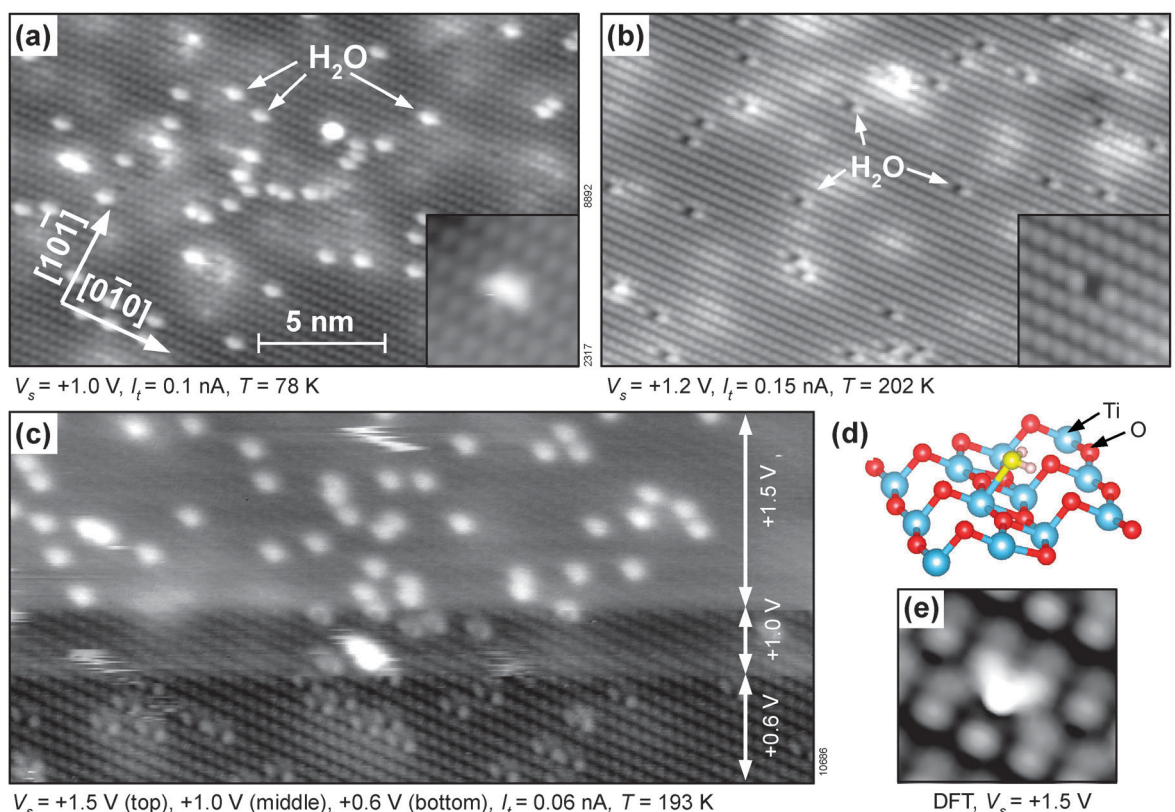


**Fig. 1** (a, b)  $20 \times 12$  nm<sup>2</sup> STM images of anatase (101) after exposure to 0.01 L  $\text{H}_2\text{O}$ , dosed at  $T_{\text{sample}} = 120$  K, scanned at (a)  $T_{\text{sample}} = 78$  K, (b)  $T_{\text{sample}} = 202$  K. (c) STM image of 0.015 L  $\text{H}_2\text{O}$  at different sample biases. The different image contrast is representative of different tip–sample distances (likely jump-to-contact of a water-covered tip in (b)) rather than different electronic states contributing to the tunneling current. (d) Structural model of an adsorbed  $\text{H}_2\text{O}$  molecule, (e) corresponding STM image calculated within the Tersoff–Hamann approximation.

becomes facile.<sup>14</sup> Possibly, a H<sub>2</sub>O molecule (or a fragment thereof) hops to the STM tip, resulting in this specific contrast.

In the STM image in Fig. 1c both image contrasts were intentionally realized. The top part of the image was obtained at  $V_{\text{Sample}} = +1.5$  V, while the two parts at the bottom were imaged at  $V_s = +1.0$  V and +0.6 V, respectively. (The slow scan direction was from bottom to top.) Here the contrast change is probably not related to the classic bias-dependence in STM; it rather originates from different tip–sample distances and so-called “jump to contact”. In the lower part of Fig. 1c, the tip (probably terminated by a water molecule) approaches the surface close enough to form a chemical bond with the sample. This is further supported by the change in contrast observed for clean parts of the sample. With a metallic tip the atomic corrugation of a clean anatase (101) surface is typically in the range of 5 to 20 pm, even when scanning the sample at a very low sample bias (<0.3 V) and thus a close tip–sample distance. Images that display the contrast shown in Fig. 1b and in the bottom of Fig. 1c exhibit typically a much larger corrugation, up to 100 pm.

When the tip scans across adsorbed H<sub>2</sub>O molecules at a higher sample bias, two subsequent changes of the molecules are induced (Fig. 2). Single H<sub>2</sub>O molecules appear as bright spots extended over several surface sites in Fig. 2a. In Fig. 2b, the upper part of the area was scanned at a high sample bias of

+2.7 V. The horizontal streaks in the STM image are indicative of tip-induced changes at the adsorbate. After the first change, the molecule appears slightly darker (see Fig. 2c; apparent height changed from 50 to 30 pm) and surrounded by a dark region. After the second change, the molecule is imaged as a dimer at the position of a Ti<sub>5c</sub> atom, surrounded by a more pronounced dark region with a radius of approximately 1 nm (see the section Oxygen below). This final configuration was previously identified as a bridging O<sub>2</sub> dimer, (O<sub>2</sub>)<sub>0</sub> in ref. 13.

Both changes occur at a similar sample bias, typically at +3 V. Likely, each of these changes corresponds to the removal of one H from the water molecule. The first tip-induced event transforms the adsorbed H<sub>2</sub>O molecule into a terminal OH group. The identification of this species as OH is further substantiated through experiments that probe the complex interaction between adsorbed H<sub>2</sub>O and O entities on anatase (101) (manuscript in preparation). The second step transforms the OH into a single O adatom, which is incorporated into the surface in the form of an O<sub>2</sub> molecule at a regular O<sub>2c</sub> lattice site, the so-called bridging (O<sub>2</sub>)<sub>0</sub> dimer.<sup>13</sup> The scanning parameters required for the tip-induced conversions are similar to those that are typically used for removing bridging hydroxyls from the rutile (110) surface.<sup>24–27</sup> Likely the hydrogen atoms are transferred to the STM tip during this process,<sup>28</sup> as the tip is biased negatively and the hydrogen atoms are positively charged.

### Carbon monoxide

Carbon monoxide binds with its C atom to a surface Ti<sub>5c</sub> (see the model in Fig. 3f). In empty-states STM images (Fig. 3) the CO appears as a bright dimer-like feature located close to the surface Ti<sub>5c</sub> atom; it looks quite similar to H<sub>2</sub>O imaged with a metallic tip (Fig. 1a). The apparent heights of CO and H<sub>2</sub>O are typically 70 and 40 pm, respectively, but distinguishing these two species from the apparent heights alone is not a very reliable method. Manipulation of the molecules *via* scanning at high bias voltages leads to a distinctly different behavior and allows a clear distinction between CO and H<sub>2</sub>O. The water molecules are difficult to move laterally with the tip; as described above, applying high bias results in abstracting the H atoms instead. In contrast, CO molecules remain stationary only when scanned at low bias (+1.0 V); when the sample bias is increased they perform lateral hops across the surface, see the Movie S1 (ESI†) and Fig. 3d.

The calculated STM image in Fig. 3e shows a single spot. Apparently this is quite different from the experimentally observed, dimer-like feature. The latter is likely due to a “wagging motion”, *i.e.*, the CO molecule tilts in the [010] direction, as shown in Fig. 4a. While the minimum-energy configuration is symmetric, the CO can be easily tilted along the [010] direction. The computed frequency of the CO wagging mode (a frustrated rotation) is only 43 (26) cm<sup>-1</sup> on the reduced (stoichiometric) surface. It is likely that the experimentally-observed, dimer-like appearance of CO molecules originates from the CO molecule oscillating between two symmetric positions. The presence of the “wagging” motion is corroborated by the appearance of a surface that was almost fully covered with

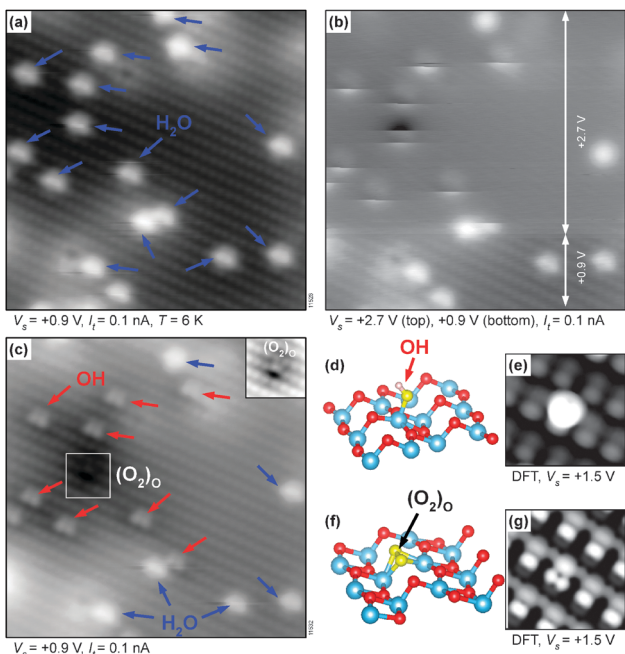


**Fig. 2** (a)–(c) Anatase (101) surface after exposure to 0.015 L H<sub>2</sub>O at  $T_{\text{sample}} = 120$  K, imaged at 6 K. (a) Before, (b) during, and (c) after imaging the upper part at  $V_{\text{sample}} = +2.7$  V. The streaks in (b) indicate structural changes induced by the electric field of the STM tip during scanning. Blue and red arrows point to H<sub>2</sub>O molecules and terminal OH groups, respectively. The circle shows an (O<sub>2</sub>)<sub>0</sub> bridging dimer [ref. 13]; the corresponding area is shown in the inset with adjusted contrast. (d, e) Structural model and calculated STM image of the terminal (OH) group. (f, g) Model and calculated STM image of the (O<sub>2</sub>)<sub>0</sub> bridging dimer.

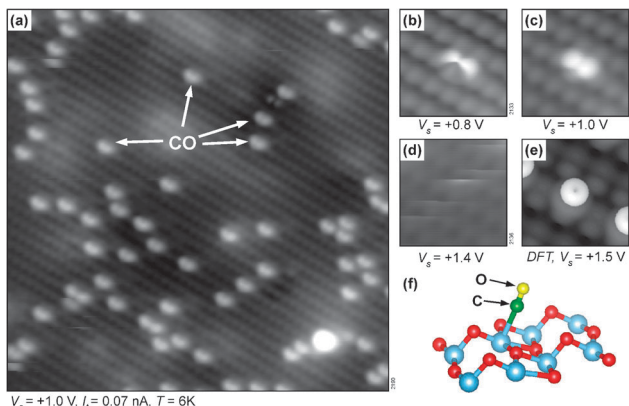


**Fig. 3** (a)  $15 \times 15 \text{ nm}^2$  STM image of the  $\text{TiO}_2$  anatase (101) surface after exposure to  $0.04 \text{ L CO}$  at  $T_{\text{sample}} = 6 \text{ K}$ . (b–d) One single CO imaged at different sample bias voltages ( $I_t = 0.1 \text{ nA}$ ). Note that scanning with higher bias voltages, as in (d), induces the CO migration across the surface, see also the Movie in the ESI.† (e) Calculated STM image. (f) Model of an adsorbed CO molecule.

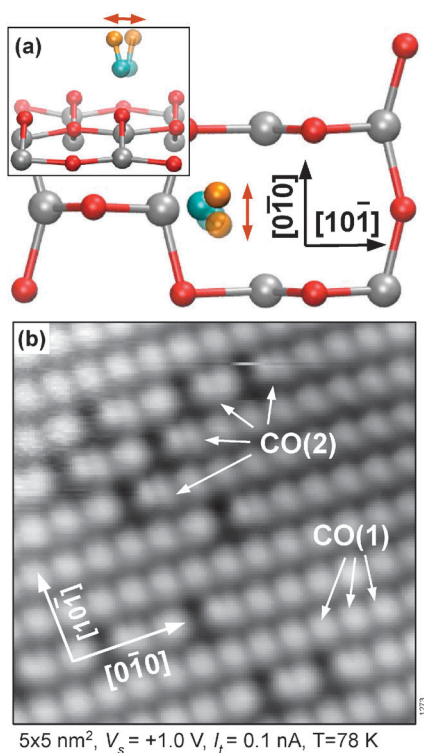


**Fig. 4** (a) Model showing the “wagging” motion of an adsorbed CO molecule. (b) STM image of an almost complete monolayer of adsorbed CO. CO molecules in densely-packed areas are imaged as single spots, marked CO(1). CO molecules with at least one missing neighbor appear twinned [marked CO(2)], which can be explained by the wagging motion depicted in (a).

CO, see Fig. 4b. Note that the anatase substrate is no longer visible; all spots in the STM image correspond to CO molecules. In areas where the CO molecules are densely packed they appear as single spots. Here the wagging motion is blocked by the neighbors and the twinning is not observed. On the other hand,

empty sites in the layer enable the wagging motion of adjacent COs, resulting in their apparent twinning.

### Oxygen

In a previous study<sup>13</sup> we identified several adsorption configurations of  $\text{O}_2$  on the anatase (101) surface. Single  $\text{O}_2$  molecules preferentially adsorb in the vicinity of subsurface extrinsic donor atoms (likely Nb atoms<sup>13</sup>) and appear as bright dimers in STM images; this configuration was named  $(\text{O}_2)_{\text{extr}}$ . As mentioned above, a single O atom is unstable in a terminal adatom configuration, and relaxes rapidly to a bridging interstitial dimer  $(\text{O}_2)_0$ .<sup>13,29</sup> The same  $(\text{O}_2)_0$  configuration forms when an  $\text{O}_2$  molecule merges with an O vacancy ( $\text{V}_0$ ), either a surface or subsurface  $\text{V}_0$ .<sup>13,30</sup> Recently, it was reported that  $\text{O}_2$  adsorbs preferentially at the steps of the anatase (101) surface.<sup>31</sup>

Again, both the  $(\text{O}_2)_{\text{extr}}$  and the  $(\text{O}_2)_0$  species show a dimer-like appearance in STM, similar to the adsorbed CO,  $\text{H}_2\text{O}$ , and OH discussed above. Some information about tip-dependent contrast of various  $\text{O}_2$  configurations was already given in the Supplement of a previous publication,<sup>13</sup> more detail is provided here and it is shown how to distinguish O-related species from these other molecules.

The bridging interstitial  $\text{O}_2$  dimer,  $(\text{O}_2)_0$ , was predicted to play an important role in the surface chemistry of anatase.<sup>32</sup> Fig. 5 shows STM images of  $(\text{O}_2)_0$  on anatase (101), taken with various tip conditions. In all cases, the  $(\text{O}_2)_0$  were prepared by tip-induced abstraction of hydrogen from water molecules. It is difficult to identify the  $(\text{O}_2)_0$ ; often it appears only as a dark spot (Fig. 5a and d). The  $(\text{O}_2)_0$  is surrounded by a dark halo; a characteristic signature of upwards band-bending induced by the negative charge localized at the excess oxygen.<sup>33</sup> This dark halo is useful for identifying the  $(\text{O}_2)_0$ . When atomic resolution is obtained, the most common contrast is the one shown in Fig. 5b. Here the  $(\text{O}_2)_0$  closely resembles the theoretical STM images calculated by the Tersoff–Hamann approach (ref. 13, also see Fig. 2g). While overall similar, the  $(\text{O}_2)_0$  in Fig. 5c has a sharp contour, indicative of tip–sample interaction. The contrast shown in Fig. 5c was frequently encountered when measuring at LHe temperature, *i.e.*, at  $T_{\text{sample}} = 6 \text{ K}$ . Fig. 5e and f show further, unusual appearances that were encountered throughout these experiments. Possibly, strong tip–surface interactions play a role in both of these imaging modes. It is noteworthy that the appearance of  $(\text{O}_2)_0$  in Fig. 5f is very similar to that of  $\text{H}_2\text{O}$  in Fig. 1b. This type of contrast was even encountered for some other adsorbates (unknown species); it seems to be a general response of the surface to a specific tip–surface interaction.

The last species discussed here is an  $\text{O}_2$  molecule adsorbed on top of a subsurface impurity atom with donor properties, the so-called  $(\text{O}_2)_{\text{extr}}$ , see Fig. 6.<sup>13</sup> The calculated adsorption energy for an  $\text{O}_2$  molecule in a direct vicinity of a subsurface Nb dopant is  $0.73 \text{ eV}$ , while it is only  $0.4 \text{ eV}$  on a clean surface of a reduced material.<sup>13</sup> The  $(\text{O}_2)_{\text{extr}}$  usually appears as a bright dimer in empty-states STM images. The  $(\text{O}_2)_{\text{extr}}$  can also exhibit various contrasts in STM images, like the other species discussed throughout this paper. The bright dimer (Fig. 6a) is the most common appearance. Another possible contrast (see Fig. 6b) has

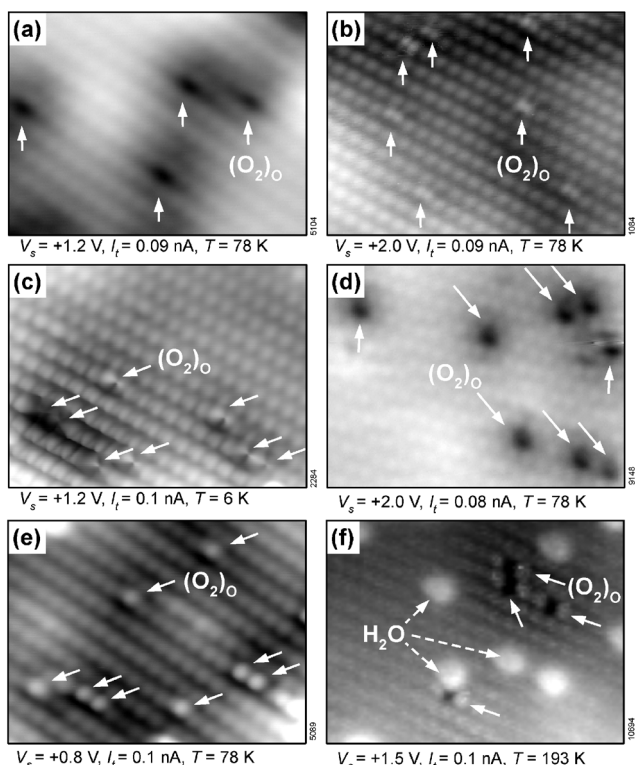


Fig. 5 (a–f) Different images of interstitial  $(\text{O}_2)_\text{O}$  molecules. The contrast in STM images depends strongly on the condition of the tip apex.

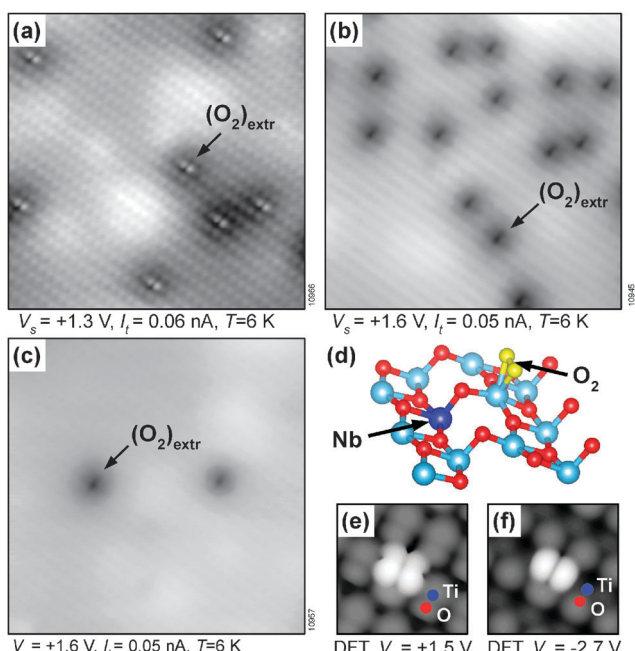


Fig. 6 (a–c) Different STM contrasts of the  $(\text{O}_2)_\text{extr}$ , i.e., an  $\text{O}_2$  adsorbed at subsurface impurity donor atoms (likely Nb). (d) Structural model of the  $(\text{O}_2)_\text{extr}$ . (e, f) Calculated empty and filled states STM images of the  $(\text{O}_2)_\text{extr}$ . Positions of substrate  $\text{Ti}_{5c}$  and  $\text{O}_{2c}$  atoms are marked.

the two bright lobes suppressed, while there is a dark depression in between. In some cases, the  $(\text{O}_2)_\text{extr}$  is only imaged as a

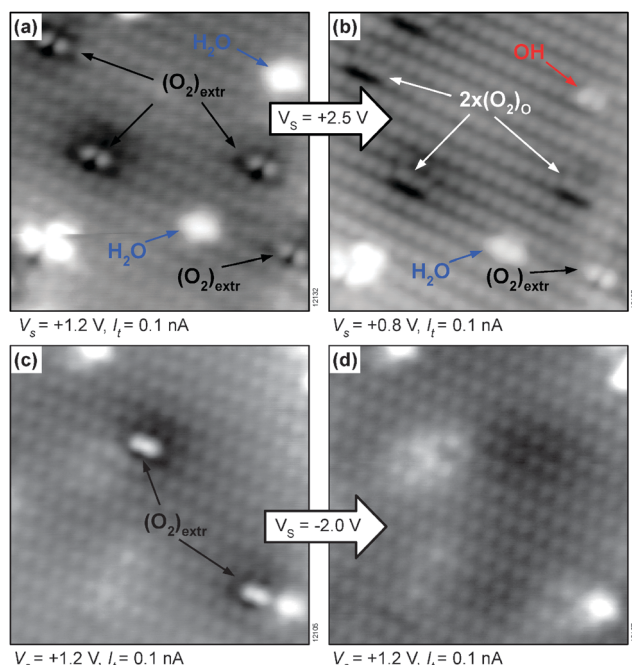


Fig. 7 Tip-induced transitions of  $(\text{O}_2)_\text{extr}$ . (a, b) The upper part of the area was scanned at  $V_\text{s} = +2.5$  V, resulting in the dissociation of the marked  $(\text{O}_2)_\text{extr}$  molecules and formation of pairs of bridging  $(\text{O}_2)_\text{O}$  interstitials. (c, d) Applying a negative bias pulse of  $-2.0$  V results in the desorption of the  $(\text{O}_2)_\text{extr}$  molecules.

dark halo caused by the upwards band-bending induced by the negative charge localized at the molecule (see Fig. 6c). This appearance is typical when the concentration of adsorbed oxygen is low (on the order of 0.001 ML).

The  $(\text{O}_2)_\text{extr}$  can be manipulated by the STM tip, see Fig. 7 and also the supplementary information of ref. 13. Fig. 7a and b show the same area of the surface before and after scanning this region with an increased sample bias of  $+2.5$  V. This results in dissociation of the  $(\text{O}_2)_\text{extr}$  molecule and formation of two adjacent  $(\text{O}_2)_\text{O}$  bridging interstitial dimers. There is no sharp threshold bias for the tip-induced dissociation; it happens for  $V_\text{sample}$  values ranging from  $+1.8$  to  $+2.5$  V. Fig. 7c and d show tip-induced desorption of the  $(\text{O}_2)_\text{extr}$  molecules that occurs when negative voltage pulses ( $-2$  V) are applied above the molecules marked in Fig. 7c.

## Discussion

All relevant adsorbates ( $\text{H}_2\text{O}$ , terminal  $\text{OH}$ ,  $\text{CO}$ ,  $\text{O}_2$ ) appear very similar in STM images. They are imaged as dimers located in the proximity of the surface  $\text{Ti}_{5c}$  atoms and oriented along the [010] direction. We have observed the same dimer-like appearance even for other adsorbed molecules not discussed here (for example methoxy). Why is the dimer-like imaging so common on the anatase (101) surface? There are two possible reasons. First, the electronic structure of some molecules simply has the dimer-like arrangement. This is for instance the case for  $(\text{O}_2)_\text{extr}$  or  $(\text{O}_2)_\text{O}$ . The second reason is illustrated for  $\text{CO}$  in Fig. 4, where it is shown both theoretically and experimentally that the  $\text{CO}$  molecule can perform

a “wagging” motion in the [010] direction. This wagging effectively results in an apparent twinning of the CO molecule in STM images. It is likely that the same wagging motion is energetically feasible for other molecules adsorbed at the anatase (101) surface.

As all the molecules shown here can exhibit a similar dimer-like appearance in STM images, a reliable chemical identification of the adsorbed species becomes complicated. It is possible to obtain certain information from the apparent heights measured in STM images, from the exact shape of the dimer, or from the band-bending observed around the adsorbed species. All these signatures are, however, dependent on the exact tip condition and it often turns out to be impossible to distinguish the single species purely from an STM image; the appearance of the adsorbed molecules is strongly tip-dependent (Fig. 1, 5 and 6). A better understanding of the STM contrasts shown throughout this paper could possibly be obtained using advanced methods for calculating STM images,<sup>12,34</sup> which include the STM tip in the calculation. As the termination of the tip can usually be only guessed, this is often not practical. The situation is particularly complex when reactions are monitored with STM, and when several species are present at the surface (or at the tip).

On the other hand, these results show that molecules can be reliably identified based on the tip–adsorbate interaction. They undergo specific, irreversible changes when a particular sample bias voltage is applied. The H<sub>2</sub>O molecules lose H when scanned at a sample bias of approximately +3 V. This converts them first into terminal OH groups and then to the bridging oxygen dimer, (O<sub>2</sub>)<sub>O</sub>. The CO molecules migrate across the surface when scanned at a somewhat elevated sample bias voltage, typically in the range from +1.4 to +2.0 V. The bridging oxygen dimer, (O<sub>2</sub>)<sub>O</sub> is very stable and no interaction with the tip was observed in a voltage range from -4 to +4 V. Finally, the (O<sub>2</sub>)<sub>extr</sub> species desorbs from the surface when a negative sample bias voltage (approximately -2 V) is applied, and dissociates at a positive bias of approximately +2.5 V. These tip-induced transformations are fully reproducible and independent of the tip condition; they prove to be the most reliable way to distinguish these adsorbates.

In our previous studies of water<sup>14</sup> and oxygen<sup>13</sup> on the anatase (101) surface, STM was used to evaluate the fundamental adsorption behavior of these molecules. In ref. 14 it was reported that water adsorbs non-dissociatively, with a binding energy of 730 meV. Diffusion of H<sub>2</sub>O was observed at a sample temperature of  $T = 190$  K. The STM images in ref. 14 correspond to the one shown in Fig. 1b. Thus, it is likely that they were taken with a water-terminated tip and affected by tip–sample interactions. A sample bias of +3.5 V was used in these published images, and the image contrast discussed in the context of Fig. 5f (where the adsorbed O<sub>2</sub> looks quite similar) asks for a careful re-evaluation. All the experiments of ref. 14 were repeated in the present study, however, and it was found that molecular H<sub>2</sub>O indeed can diffuse in the temperature range from 180 to 220 K, while (O<sub>2</sub>)<sub>O</sub> is immobile, validating the conclusions drawn in this earlier publication.

The adsorption of O<sub>2</sub> was treated in ref. 13. One of the adsorption configurations reported here, (O<sub>2</sub>)<sub>ads</sub>, was assigned

as an O<sub>2</sub> molecule adsorbed above a subsurface oxygen vacancy. Its appearance in STM is exactly the same as the H<sub>2</sub>O molecules shown in Fig. 1a, however. Also the tip-induced changes in Fig. 2 are identical to those reported in ref. 13. Thus the interpretation of the first tip-induced change as a transition of a superoxo to a peroxy configuration of O<sub>2</sub>, and the second transition as merging the O<sub>2</sub> molecule with a subsurface vacancy, need to be revoked. Detailed experiments with water adsorption show that these species, interpreted as (O<sub>2</sub>)<sub>ads</sub>, are water molecules which originate from residual H<sub>2</sub>O present in the STM chamber or displaced from the walls of the UHV chamber by the O<sub>2</sub> molecules. This raises the question which of the O<sub>2</sub>-related species is the key intermediate for the catalytic reactions on the anatase (101) surface. Here we have shown that the (O<sub>2</sub>)<sub>O</sub> can be created *via* tip-induced abstraction of hydrogen from adsorbed water. In ref. 13 we have argued that the (O<sub>2</sub>)<sub>O</sub> configuration could be created by merging a subsurface oxygen vacancy with an adsorbed O<sub>2</sub> molecule. After dosing oxygen on a clean anatase (101) surface (at  $T = 105$  K), we can observe 0.001 to 0.01 ML of single bridging (O<sub>2</sub>)<sub>O</sub> dimers. This indicates that (i) concentration of subsurface oxygen vacancies is probably low when compared to the concentration of surface oxygen vacancies on the rutile (110); and (ii) direct reaction of O<sub>2</sub> with subsurface V<sub>O</sub>'s may not be the main reaction pathway in catalytic reactions on anatase.

## Conclusions

Simple molecules (H<sub>2</sub>O, CO, O<sub>2</sub>) adsorbed on the TiO<sub>2</sub> anatase (101) surface show a wide variety of appearances in STM images that are strongly influenced by the tip condition. Here it was discussed which contrast types are related to a metallic, non-interacting tip and which contrasts are likely influenced by the interaction between the tip and the surface.

For clean tips, the adsorbates considered here can show a similar appearance in STM images – a dimer parallel to the [010] direction. This complicates identification of these species in STM images and has, in fact, lead to erroneous conclusions in a previous paper by this group.<sup>13</sup> On the other hand, the present results show that each of these adsorbed species has a specific response when scanned at a higher sample bias. This tip–adsorbate interaction, while often destructive for a few, selected molecules, provides a reliable identification and constitutes a novel, simple, and efficient tool to distinguish between different adsorbed molecules and reaction products. This method is generally applicable and should be helpful for exploring photon-, temperature-, and field-induced surface chemistry at the atomic level.

## Acknowledgements

This work was supported by the ERC Advanced Grant “Oxide-Surfaces” (experiments) and by DoE-BES, Division of Chemical Sciences, Geosciences and Biosciences under Award DE-FG02-12ER16286 (computations). We used resources of the National

Energy Research Scientific Computing Center (DoE Contract No. DE-AC02-05CH11231).

## References

- 1 A. Linsebigler, G. Lu and J. J. T. Yates, *Chem. Rev.*, 1995, **95**, 735–798.
- 2 M. A. Henderson, *Surf. Sci. Rep.*, 2011, **66**, 185–297.
- 3 M. Grätzel, *Nature*, 2001, **414**, 338–344.
- 4 Y. Furubayashi, T. Hitosugi, Y. Yamamoto, K. Inaba, G. Kinoda, Y. Hirose, T. Shimada and T. Hasegawa, *Appl. Phys. Lett.*, 2005, **86**, 252101.
- 5 K. Szot, M. Rogala, W. Speier, Z. Klusek, A. Besmehn and R. Waser, *Nanotechnology*, 2011, **22**, 254001.
- 6 U. Diebold, *Surf. Sci. Rep.*, 2003, **48**, 53–229.
- 7 M. Lazzari, A. Vittadini and A. Selloni, *Phys. Rev. B: Condens. Matter Mater. Phys.*, 2001, **63**, 155409.
- 8 M. Setvin, C. Franchini, X. Hao, M. Schmid, A. Janotti, M. Kaltak, C. G. Van de Walle, G. Kresse and U. Diebold, *Phys. Rev. Lett.*, 2014, **113**, 086402.
- 9 C. L. Pang, R. Lindsay and G. Thornton, *Chem. Soc. Rev.*, 2008, **37**, 2328–2353.
- 10 T. Luttrell, S. Halpegamage, J. Tao, A. Kramer, E. Sutter and M. Batzill, *Sci. Rep.*, 2014, **4**, 4043.
- 11 G. H. Enevoldsen, H. P. Pinto, A. S. Foster, M. C. R. Jensen, A. Kühnle, M. Reichling, W. A. Hofer, J. V. Lauritsen and F. Besenbacher, *Phys. Rev. B: Condens. Matter Mater. Phys.*, 2008, **78**, 045416.
- 12 R. Bechstein, C. Gonzalez, J. Schütte, P. Jelinek, R. Perez and A. Kühnle, *Nanotechnology*, 2009, **20**, 505703.
- 13 M. Setvin, U. Aschauer, P. Scheiber, Y. F. Li, W. Hou, M. Schmid, A. selloni and U. Diebold, *Science*, 2013, **341**, 988–991.
- 14 Y. He, A. Tilocca, O. Dulub, A. Selloni and U. Diebold, *Nat. Mater.*, 2009, 585–589.
- 15 O. Dulub and U. Diebold, *J. Phys.: Condens. Matter*, 2010, **22**, 084014.
- 16 M. Setvin, B. Daniel, V. Mansfeldova, L. Kavan, P. Scheiber, M. Fidler, M. Schmid and U. Diebold, *Surf. Sci.*, 2014, **626**, 61–67.
- 17 J. P. Perdew, K. Burke and M. Ernzerhof, *Phys. Rev. Lett.*, 1996, **77**, 3865–3868.
- 18 V. I. Anisimov, J. Zaanen and O. K. Andersen, *Phys. Rev. B: Condens. Matter Mater. Phys.*, 1991, **44**, 943.
- 19 P. Giannozzi, S. Baroni, N. Bonini, M. Calandra, R. Car, C. Cavazzoni, D. Ceresoli, G. L. Chiarotti, M. Cococcioni, I. Dabo, A. Dal Corso, S. de Gironcoli, S. Fabris, G. Fratesi, R. Gebauer, U. Gerstmann, C. Gougaussis, A. Kokalj, M. Lazzari, L. Martin-Samos, N. Marzari, F. Mauri, R. Mazzarello, S. Paolini, A. Pasquarello, L. Paulatto, C. Sbraccia, S. Scandolo, G. Sclauzero, A. P. Seitsonen, A. Smogunov, P. Umari and R. M. Wentzcovitch, *J. Phys.: Condens. Matter*, 2009, **21**, 395502.
- 20 D. Vanderbilt, *Phys. Rev. B: Condens. Matter Mater. Phys.*, 1990, **41**, 7892–7895.
- 21 M. Cococcioni and S. de Gironcoli, *Phys. Rev. B: Condens. Matter Mater. Phys.*, 2005, **71**, 035105.
- 22 G. Henkelman, B. P. Uberuaga and H. Jónsson, *J. Chem. Phys.*, 2000, **113**, 9901–9904.
- 23 G. S. Herman, Z. Dohnalek, N. Ruzycki and U. Diebold, *J. Phys. Chem. B*, 2003, **107**, 2788–2795.
- 24 C. L. Pang, O. Bikonda, D. S. Humphrey, A. C. Papageorgiou, G. Cabailh, R. Ithnin, Q. Chen, C. A. Muryn, H. Onishi and G. Thornton, *Nanotechnology*, 2006, **17**, 5397–5405.
- 25 S. Wendt, R. Schlaub, J. Matthiesen, E. K. Vestergaard, R. Wahlström, M. D. Rasmussen, P. Thostrup, L. M. Molina, E. Laegsgaard, B. Hammer and F. Besenbacher, *Surf. Sci.*, 2005, 226–245.
- 26 O. Bikonda, C. L. Pang, R. Ithnin, C. A. Muryn, H. Onishi and G. Thornton, *Nat. Mater.*, 2006, **5**, 189–192.
- 27 J. Lee, D. C. Sorescu, X. Deng and K. D. Jordan, *J. Phys. Chem. Lett.*, 2012, **4**, 53–57.
- 28 T. Minato, M. Kawai and Y. Kim, *J. Mater. Res.*, 2012, **27**, 2237–2240.
- 29 Y.-F. Li, U. Aschauer, J. Chen and A. Selloni, *Acc. Chem. Res.*, 2014, DOI: 10.1021/ar400312t.
- 30 P. Scheiber, M. Fidler, O. Dulub, M. Schmid, U. Diebold, W. Hou, U. Aschauer and A. Selloni, *Phys. Rev. Lett.*, 2012, **109**, 136103.
- 31 M. Setvin, X. Hao, B. Daniel, J. Pavělec, Z. Novotny, G. S. Parkinson, M. Schmid, G. Kresse, C. Franchini and U. Diebold, *Angew. Chem., Int. Ed.*, 2014, **53**, 4714–4716.
- 32 Y.-F. Li, Z.-P. Liu, L. Liu and W. Gao, *J. Am. Chem. Soc.*, 2010, **132**, 13008–13015.
- 33 P. Ebert, *Surf. Sci. Rep.*, 1999, **33**, 121–303.
- 34 A. Yurtsever, D. Fernandez-Torre, C. Gonzalez, P. Jelinek, P. Pou, Y. Sugimoto, M. Abe, R. Perez and S. Morita, *Phys. Rev. B: Condens. Matter Mater. Phys.*, 2012, **85**, 125416.